International Journal of Solids and Structures 190 (2020) 47–57

Contents lists available at ScienceDirect

International Journal of Solids and Structures

journal homepage: www.elsevier.com/locate/ijsolstr

On the solution of the purely nonlocal theory of beam elasticity as a limiting case of the two-phase theory

Gennadi Mikhasev[a], Andrea Nobili[b,*]

[a] Department of Bio- and Nanomechanics, Belarusian State University, 4 Nezavisimosti Ave., Minsk 220030, Belarus
[b] Engineering Department "Enzo Ferrari", Università Degli Studi di Modena e Reggio Emilia, Modena 41125, Italy

ARTICLE INFO

Article history:
Received 8 August 2019
Revised 3 October 2019
Accepted 21 October 2019
Available online 31 October 2019

Keywords:
Two-phase nonlocal elasticity
Nonlocal theory of elasticity
Asymptotic method
Free vibrations

ABSTRACT

In the recent literature stance, purely nonlocal theory of elasticity is recognized to lead to ill-posed problems. Yet, we show that, for a beam, a meaningful energy bounded solution of the purely nonlocal theory may still be defined as the limit solution of the two-phase nonlocal theory. For this, we consider the problem of free vibrations of a flexural beam under the two-phase theory of nonlocal elasticity with an exponential kernel, in the presence of rotational inertia. After recasting the integro-differential governing equation and the boundary conditions into purely differential form, a singularly perturbed problem is met that is associated with a pair of end boundary layers. A multi-parametric asymptotic solution in terms of size-effect and local fraction is presented for the eigenfrequencies as well as for the eigenforms for a variety of boundary conditions. It is found that, for simply supported end, the weakest boundary layer is formed and, surprisingly, rotational inertia affects the eigenfrequencies only in the classical sense. Conversely, clamped and free end conditions bring a strong boundary layer and eigenfrequencies are heavily affected by rotational inertia, even for the lowest mode, in a manner opposite to that brought by nonlocality. Remarkably, all asymptotic solutions admit a well defined and energy bounded limit as the local fraction vanishes and the purely nonlocal model is retrieved. Therefore, we may define this limiting case as the proper solution of the purely nonlocal model for a beam. Finally, numerical results support the accuracy of the proposed asymptotic approach.

1. Introduction

The classical linear theory of elasticity suffers from the well known defect of not encompassing an internal length scale, which feature gives rise to self-similar predictions. Yet, any real material possesses an internal microstructure and some characteristic length thereof. Consequently, classical elasticity may be assumed as a suitable model inasmuch as the physical phenomena of interest occur at a scale much greater than the internal characteristic length of the material. Failure to meet this condition is effectively demonstrated by, for instance, the singular stress field at the tip of a crack and by the non-dispersive nature of wave propagation. Extensions of classical elasticity have been proposed, in the form of generalized continuum mechanics (GCM), in an attempt to remediate these shortfalls. An excellent historical overview of GCM, together with extensive bibliographic details, may be found in (Maugin, 2011). Among GCM theories, we mention the theory of micro-polar elasticity (Cosserat and Cosserat, 1909; Dai., 2003; Pietraszkiewicz and Eremeyev, 2009), the couple-stress and strain-gradient elasticity theories (Yang et al., 2002; Nobili et al., 2019) and the nonlocal theory of elasticity (Eringen, 1984). In particular, following (Eringen, 1984), "linear theory of nonlocal elasticity, which has been proposed independently by various authors [...], incorporates important features of lattice dynamics and yet it contains classical elasticity in the long wave length limit". Nonlocal elasticity is based on the idea that the stress state at a point is a convolution over the whole body of an attenuation function (sometimes named kernel or nonlocal modulus) with the strain field (Wang et al., 2016). Although several attenuation functions may be considered, they need to comply with some important properties which warrant that (a) classical elasticity is reverted to in the limit of zero length scale and that (b) normalization is satisfied (Eringen, 1983; Koutsoumaris et al., 2017). As an example, Helmholtz and bi-Helmholtz kernels have been widely used in 1-D problems, their name stemming from the differential operators they are Green's function of (Eringen, 2002; Koutsoumaris and Eptaimeros, 2018). In (Eptaimeros et al., 2016), a variational argument is adopted to de-

* Corresponding author.
E-mail addresses: mikhasev@bsu.by (G. Mikhasev), andrea.nobili@unimore.it (A. Nobili).

https://doi.org/10.1016/j.ijsolstr.2019.10.022
0020-7683/

duce the governing equations for a purely nonlocal Euler-Bernoulli beam, whose eigenfrequencies are numerically investigated.

Since nonlocal elasticity naturally leads to integro-differential equations whose solution is most often impractical, an equivalent differential nonlocal model (EDNM) was developed in Eringen (1983). In such differential form, nonlocal elasticity has been extensively applied to study elastodynamics of beams and shells as described in the recent review (Eltaher et al., 2016) and with special emphasis on the application to nanostructures (Rafii-Tabar et al., 2016). Generally, EDNM leads to interesting mechanical effects, such as increased deflections and decreased buckling loads and natural frequencies (softening effect), when compared to classical elasticity. However, a number of pathological results have also emerged, which are often referred to as paradoxes (Lu et al., 2006; Fernández-Sáez et al., 2016; Koutsoumaris and Eptaimeros, 2018). For instance, for a cantilever beam under point loading, nonlocality brings no effect (Peddieson et al., 2003; Wang and Liew, 2007; Challamel and Wang, 2008; Koutsoumaris et al., 2017). It should be remarked that many studies based on the EDNM employ boundary conditions in terms of macroscopic stresses, i.e. in classical form, and therefore they disregard the important effect of the boundary through nonlocality. Although this approach may be still adopted for long structures or in the case of localized deformations occurring away from the boundaries (Mikhasev, 2014; Mikhasev and Botogova, 2016), it is generally inaccurate.

Very recently, Romano et al. (2017) claimed that Eringen's purely nonlocal model (PNLM) leads to ill-posed problems for the differential form of the model is consistent inasmuch as an extra pair of boundary conditions, termed constitutive, is satisfied (see also Mahmoud, 2017). In (Eringen, 1984, Eq. (6.4)) and in (Altan, 1989), a two-phase nonlocal model (TPNL) was introduced, within the context of 3D elasticity, which combines, according to the theory of mixtures, purely nonlocal elasticity with classical elasticity, by means of the volume fractions ξ_1 and $\xi_2 = 1-\xi_1$. This model is immune from the inconsistencies of the PNLM and it has been adopted to solve the problem of static bending (Wang et al., 2016) and buckling (Zhu et al., 2017) of Euler-Bernoulli (E-B) beams. Static axial deformation of a beam is considered in (Pisano and Fuschi, 2003; Zhu and Dai, 2012), while semi-analytical solutions for the combined action of axial and flexural static loadings is given in (Meng et al., 2018). Axial and flexural free vibrations of beams have also been considered in (Mikhasev et al., 2018) and in (Fernández-Sáez and Zaera, 2017). In these works, either the TPNM is solved numerically or it is reduced, by adopting the solution presented in (Polyanin and Manzhirov, 1998), to an equivalent higher-order purely differential model with a pair of extra boundary conditions. Despite this reduction, the differential model is still difficult to analyse, especially in the neighbourhood of the PNLM, that is for ξ_1 small. In this respect, we believe that the asymptotic approach may be put to great advantage in predicting the mechanical behaviour of nanoscale structures for a vanishingly small ξ_1 (Zhu et al., 2017; Mikhasev et al., 2018).

In this paper, we consider free vibrations of a flexural beam taking into account rotational inertia (Rayleigh beam), within the TPNM and having assumed the Helmholtz attenuation function. The integro-differential model is reduced to purely differential form with an extra pair of boundary conditions. Spotlight is set on developing asymptotic solutions valid for small microstructure and/or little local fraction. These solutions feature a pair of boundary layers located at the beam ends, whose strength depends on the constraining conditions. Numerical results support the accuracy of the expansions. Most remarkably, the asymptotic approach allows to investigate the behaviour of the solution in the neighbourhood of the PNLM, where the expansions are non-uniform. Nonetheless, they admit a perfectly meaningful, energy bounded limit, which may be taken as the solution of the PNLM. We point out that the existence of such limit has been observed numerically in (Fernández-Sáez et al., 2016) for free-free end conditions.

2. Problem formulation

2.1. Governing equations

For a flexural beam, vertical equilibrium gives

$$\rho S\frac{\partial^2 v}{\partial t^2} = \frac{\partial \hat{Q}}{\partial x} + \hat{q}(x) \tag{1}$$

while rotational equilibrium lends

$$J\frac{\partial^2 \varphi}{\partial t^2} = -\frac{\partial \hat{M}}{\partial x} + \hat{Q}. \tag{2}$$

Here, $v = v(x,t)$ is the vertical displacement, $\hat{Q}$ and $\hat{M}$ are the *dimensional* shearing force and the bending moment, respectively, ρ is the mass density per unit volume, $J = \rho I$ is the mass second moment of inertia per unit length of the beam, that is proportional to the second moment of area *I*, *S* is the cross-sectional area and $\hat{q}(x)$ the vertical applied load. Assuming that the beam is homogeneous and prismatic, Eqs. (1) and (2) give

$$\frac{\partial^2 \hat{M}}{\partial x^2} - \rho S\frac{\partial^2 v}{\partial t^2} + J\frac{\partial^4 v}{\partial x^2 \partial t^2} + \hat{q} = 0, \tag{3}$$

that governs transverse vibrations of flexural beams accounting for rotational inertia. In the following, we take $\hat{q} \equiv 0$. In the mixed nonlocal theory (MNLT) of elasticity, we have (Fernández-Sáez and Zaera, 2017)

$$\hat{M} = -EI\left(\xi_1 \frac{\partial^2 v}{\partial x^2} + \xi_2 \int_0^L K(|x-\hat{x}|,\kappa)\frac{\partial^2 v}{\partial \hat{x}^2} d\hat{x}\right), \tag{4}$$

where EI is the beam flexural rigidity, L the beam length and $K(|x-\hat{x}|,\kappa)$ is the kernel or attenuation function. The kernel is positive, symmetric, it rapidly decays away from x and it satisfies the normalization condition

$$\int_{\mathbb{R}} K(|x-\hat{x}|,\kappa)\mathrm{d}\hat{x} = 1.$$

The constitutive Eq. (4) is also obtained from consideration of a more general form of kernel discussed in (Koutsoumaris et al., 2017). The nonlocal parameter $\kappa = e_0 a$ depends on the scale coefficient e_0 as well as on the internal length scale *a*. ξ_1 and ξ_2 take up the role of volume fractions and they represent, respectively, the local and the nonlocal phase ratios, such that $\xi_1 + \xi_2 = 1$ and $\xi_1\xi_2 \geq 0$. When $\xi_1 = 0$, Eq. (4) degenerates into the purely nonlocal model (PNLM), while, in contrast, the case $\xi_1 = 1$ corresponds to classical local elasticity.

In what follows, we consider the Helmholtz kernel

$$K(|x-\hat{x}|,\kappa) = \frac{1}{2\kappa}\exp\left(-\frac{|x-\hat{x}|}{\kappa}\right), \tag{5}$$

which is frequently used for 1D problems (indeed, it is named *special kernel* in Romano et al., 2017). We note that for the Helmholtz kernel the following transformations are valid

$$\frac{\mathrm{d}}{\mathrm{d}s}\int_0^1 \mathrm{e}^{-\frac{|s-\hat{s}|}{\varepsilon}} y(\hat{s})\mathrm{d}\hat{s} = \frac{1}{\varepsilon}\left[\mathrm{e}^{\frac{s}{\varepsilon}}\int_s^1 \mathrm{e}^{-\frac{\hat{s}}{\varepsilon}} y(\hat{s})\mathrm{d}\hat{s} - \mathrm{e}^{-\frac{s}{\varepsilon}}\int_0^s \mathrm{e}^{\frac{\hat{s}}{\varepsilon}} y(\hat{s})\mathrm{d}\hat{s}\right], \tag{6}$$

and

$$\frac{\mathrm{d}^2}{\mathrm{d}s^2}\int_0^1 \mathrm{e}^{-\frac{|s-\hat{s}|}{\varepsilon}} y(\hat{s})\mathrm{d}\hat{s} = \frac{1}{\varepsilon^2}\int_0^1 \mathrm{e}^{-\frac{|s-\hat{s}|}{\varepsilon}} y(\hat{s})\mathrm{d}\hat{s} - \frac{2}{\varepsilon}y(s). \tag{7}$$

In particular, Eq. (7) corresponds to (Romano et al., 2017), Eq. (6) and it may be rewritten as

$$\int_0^1 \left[\varepsilon^2 \frac{\mathrm{d}^2 K(|s-\hat{s}|,\varepsilon)}{\mathrm{d}s^2} - K(|s-\hat{s}|,\varepsilon) + \delta(|s-\hat{s}|)\right] y(\hat{s})\mathrm{d}\hat{s} = 0,$$

whereupon $K(|s-\hat{s}|,\varepsilon)$ is the Green's function of the singularly perturbed operator $\mathbf{H}_\varepsilon = 1-\varepsilon^2\frac{\mathrm{d}^2}{\mathrm{d}s^2}$. It is trivial matter to prove impulsivity, i.e. $\lim_{\varepsilon\to 0} K(|s-\hat{s}|,\varepsilon) = \delta(s-\hat{s})$, where $\delta(s)$ is Dirac's delta function. Furthermore, we observe that Eq. (6), evaluated at the beam ends $s = 0, 1$ and for $\xi = 0$, lends the constitutive boundary conditions (Romano et al., 2017), Eq. (5)

$$\frac{\mathrm{d}\hat{M}}{\mathrm{d}s}(0) = \varepsilon^{-1}\hat{M}(0), \quad \text{and} \quad \frac{\mathrm{d}\hat{M}}{\mathrm{d}s}(1) = -\varepsilon^{-1}\hat{M}(1).$$

Thus, the constitutive boundary conditions are really the expression, on the domain boundary, of a general feature of the solution that is related to the integral operator (4).

Introducing the dimensionless axial co-ordinate $s = x/L$ and under the assumption of time-harmonic motion, we write

$$\left\{v, \hat{M}, \hat{Q}\right\} = \left\{w(s), \frac{EI}{L}M(s), \frac{EI}{L^2}Q(s)\right\}\exp(\imath\omega t),$$

where $\imath$ is the imaginary unit. Upon multiplying throughout by L^4/EI, Eq. (3) may be turned in dimensionless form

$$\xi_1\frac{\mathrm{d}^4 w}{\mathrm{d}s^4} + \left(\lambda^4\theta - \varepsilon^{-2}\xi_2\right)\frac{\mathrm{d}^2 w}{\mathrm{d}s^2} + \frac{\xi_2}{2\varepsilon^3}\int_0^1 \exp\left(-\frac{|\hat{s}-s|}{\varepsilon}\right)\frac{\mathrm{d}^2 w(\hat{s})}{\mathrm{d}\hat{s}^2}\mathrm{d}\hat{s} - \lambda^4 w = 0. \tag{8}$$

Here, use have been made of Eqs. (4) and (5) and we have let the dimensionless ratios

$$\theta = \frac{J}{\rho S L^2} = \left(\frac{r_A}{L}\right)^2, \quad \lambda^4 = \frac{\rho S L^4\omega^2}{EI}, \tag{9}$$

together with the microstructure parameter

$$\varepsilon = \frac{\kappa}{L} \ll 1.$$

Here r_A is the radius of gyration. Clearly, θ plays the role of an aspect ratio squared and ε is a *scale effect*. Assuming $w \in C^6[0, 1]$, twice differentiating Eq. (8), making use of Eq. (7) and then subtracting the original Eq. (8), we get the governing equation in purely differential form

$$\varepsilon^2\xi\frac{\mathrm{d}^6 w}{\mathrm{d}s^6} - \left(1-\varepsilon^2\theta\lambda^4\right)\frac{\mathrm{d}^4 w}{\mathrm{d}s^4} - \lambda^4\left(\varepsilon^2+\theta\right)\frac{\mathrm{d}^2 w}{\mathrm{d}s^2} + \lambda^4 w = 0, \tag{10}$$

where, hereinafter, we adopt the shorthand $\xi = \xi_1$. Eq. (10) is a singularly perturbed ODE (Kevorkian and Cole, 1996), with respect to the small parameter $\varepsilon\sqrt{\xi}$.

2.2. Boundary conditions

Eq. (10) is supplemented by suitable boundary conditions (BCs) at the ends. For clamped ends (C-C conditions), we have two pairs of kinematical conditions

$$w(0) = w'(0) = 0, \tag{11a}$$

$$w(1) = w'(1) = 0. \tag{11b}$$

For simply supported (S-S) ends

$$w(0) = 0, M(0) = \xi w''(0) + M_0 = 0, \tag{12a}$$

$$w(1) = 0, M(1) = \xi w''(1) + M_1 = 0, \tag{12b}$$

having let

$$M_0 = \frac{1-\xi}{2\varepsilon}\int_0^1 \mathrm{e}^{-\frac{\hat{s}}{\varepsilon}} w''(\hat{s})\mathrm{d}\hat{s}, \quad M_1 = \frac{1-\xi}{2\varepsilon}\mathrm{e}^{-\frac{1}{\varepsilon}}\int_0^1 \mathrm{e}^{\frac{\hat{s}}{\varepsilon}} w''(\hat{s})\mathrm{d}\hat{s}. \tag{13}$$

For free-free (F-F) ends, one has

$$M(0) = 0, Q(0) = \xi w'''(0) + \theta\lambda^4 w'(0) + \varepsilon^{-1}M_0 = 0, \tag{14a}$$

$$M(1) = 0, Q(1) = \xi w'''(1) + \theta\lambda^4 w'(1) - \varepsilon^{-1}M_1 = 0. \tag{14b}$$

The nonlocal end bending moments (13) may be rewritten in differential form with the help of the original integro-differential Eq. (8):

$$M_0 = -\varepsilon^2\xi w^{iv}(0) + \left[1-\xi-\varepsilon^2\theta\lambda^4\right]w''(0) + \varepsilon^2\lambda^4 w(0), \tag{15a}$$

$$M_1 = -\varepsilon^2\xi w^{iv}(1) + \left[1-\xi-\varepsilon^2\theta\lambda^4\right]w''(1) + \varepsilon^2\lambda^4 w(1). \tag{15b}$$

Consequently, the BCs may be recast in differential form through

$$M(0) = w''(0) + \varepsilon^2 N_0, \tag{16a}$$

$$M(1) = w''(1) + \varepsilon^2 N_1, \tag{16b}$$

$$Q(0) = \xi w'''(0) + \theta\lambda^4 w'(1) + \varepsilon^{-1}M_0, \tag{16c}$$

$$Q(1) = \xi w'''(1) + \theta\lambda^4 w'(1) - \varepsilon^{-1}M_1, \tag{16d}$$

where, making use of the connections (6,7), we have

$$N_0 = \varepsilon^{-2}\left(\xi_2 w''(0) - M_0\right) = -\xi w^{iv}(0) - \theta\lambda^4 w''(0) + \lambda^4 w(0), \tag{17a}$$

$$N_1 = \varepsilon^{-2}\left(\xi_2 w''(1) - M_1\right) = -\xi w^{iv}(1) - \theta\lambda^4 w''(1) + \lambda^4 w(1). \tag{17b}$$

Besides, to rule out spurious solutions which may have appeared owing to double differentiation, we introduce a pair of additional BCs. Indeed, evaluating at the beam ends the original governing Eq. (8), differentiated once with respect to s, one arrives at

$$\varepsilon^3\xi w^v(0) - \varepsilon^2\xi w^{iv}(0) - \left(1-\xi-\varepsilon^2\theta\lambda^4\right)\left[\varepsilon w'''(0) - w''(0)\right] - \varepsilon^3\lambda^4 w'(0) + \varepsilon^2\lambda^4 w(0) = 0, \tag{18a}$$

$$\varepsilon^3\xi w^v(1) + \varepsilon^2\xi w^{iv}(1) - \left(1-\xi-\varepsilon^2\theta\lambda^4\right)\left[\varepsilon w'''(1) + w''(1)\right] - \varepsilon^3\lambda^4 w'(1) - \varepsilon^2\lambda^4 w(1) = 0. \tag{18b}$$

Dropping rotational inertia, the additional boundary conditions (18) coincide with the *constitutive boundary conditions* recently obtained by (Fernández-Sáez and Zaera, 2017, Eqs. (59) and (60)), provided that we replace our ε and λ^4 with their h and λ_w, respectively. However, it should be remarked that in Fernández-Sáez and Zaera (2017) the original integro-differential problem is reduced to the equivalent differential form extending to dynamics the original argument developed in (Wang et al., 2016) for statics. Such argument takes advantage of a result presented in (Polyanin and Manzhirov, 2008), which really applies to inhomogeneous integral equations with a given right-hand side. In the case of dynamics, however, this right-hand side is a problem unknown, for it is really an acceleration term, and therefore the applicability of the reduction formula is questionable.

3. Exact solution of the boundary-value problems

The general solution of the ODE (10) is

$$w(s) = \sum_{j=1}^{6} c_j \exp\left(b_j s\right),$$

where the constants b_j are the roots of the characteristic polynomial in ζ

$$\varepsilon^2\xi\zeta^6 - \left(1-\varepsilon^2\theta\lambda^4\right)\zeta^4 - \left(\varepsilon^2+\theta\right)\lambda^4\zeta^2 + \lambda^4 = 0. \tag{19}$$

As detailed in (Smirnov, 1964; Nobili and Lanzoni, 2010), this bi-cubic may be turned in canonical form by the substitution $Z = \zeta^2 - Z_0$, it being $Z_0 = (1-\varepsilon^2\theta\lambda^4)/(3\varepsilon^2\xi)$. Hence, Eq. (19) becomes

$$Z^3 - pZ - q = 0,$$

where

$$p = \left(\xi\varepsilon^2\right)^{-1}\left[\frac{\left(\lambda^4\theta\varepsilon^2-1\right)^2}{3\xi\varepsilon^2} + \lambda^4\left(\theta+\varepsilon^2\right)\right] > 0,$$

$$q = -\left(\xi\varepsilon^2\right)^{-1}\left[\lambda^4 + \frac{\lambda^4\left(\theta+\varepsilon^2\right)\left(\lambda^4\theta\varepsilon^2-1\right)}{3\xi\varepsilon^2} + \frac{2\left(\lambda^4\theta\varepsilon^2-1\right)^3}{27\xi^2\varepsilon^4}\right].$$

This polynomial possesses three real roots provided that

$$\Delta = \frac{q^2}{4} - \frac{p^3}{27} < 0$$

and indeed, for $\varepsilon\sqrt{\xi} \ll 1$, we get, to leading order,

$$\Delta = -\lambda^4\frac{4+\theta^2\lambda^4}{108(\xi\varepsilon^2)^4}.$$

Besides, we have, at leading order,

$$q = \frac{2}{27(\xi\varepsilon^2)^3}$$

and $q > 0$, whereupon out of the three real roots, two, say $Z_3 < Z_2$, are negative and one, say Z_1, is positive. Upon reverting to the original variable ζ, we see that $\zeta_3^2 < 0 < \zeta_2^2 < \zeta_1^2$. Indeed, we get the leading order solutions (the sign is immaterial)

$$\zeta_1 = \frac{1}{\varepsilon\sqrt{\xi}}, \quad \zeta_2 = \alpha, \quad \zeta_3 = \imath\beta,$$

with

$$\alpha = \lambda\sqrt{-\frac{1}{2}\theta\lambda^2 + \sqrt{1+\frac{\theta^2\lambda^4}{4}}}, \tag{20a}$$

$$\beta = \lambda\sqrt{\frac{1}{2}\theta\lambda^2 + \sqrt{1+\frac{\theta^2\lambda^4}{4}}}, \tag{20b}$$

whence $\zeta_{1,2}$ convey an exponential solution, while ζ_3 is related to an oscillatory contribution. It is worth noticing that ζ_1 blows up as $(\varepsilon\sqrt{\xi}) \to 0$, that is for a vanishingly small scale effect or in the purely nonlocal situation. Indeed, this very root accounts for the edge effect in this problem and it describes a boundary layer.

We observe that, in general, the frequency equation for the ODE (10), subject to suitable boundary conditions, appears in transcendental form

$$F(\lambda;\xi,\varepsilon) = 0,$$

wherein λ is the sought-for eigenvalue. The numerical solution of this equation is not straightforward matter, especially for very small values of the local fraction ξ, see e.g., Fernández-Sáez and Zaera (2017) and Wang et al. (2016) where plots are given for $\xi > 0.1$ and $\xi > 0.05$, respectively. Indeed, when looking for the numerical roots of (19), we observe, after (Smirnov, 1964), that the transformation to canonical form lends a considerable numerical advantage over Cardano's formulas, in that it provides purely real solutions. Conversely, Cardano's formulas are likely to introduce a very small spurious imaginary component, which is most likely the cause of the numerical difficulty encountered in the literature when dealing with small ξ.

To estimate the eigenvalue λ for any ξ and, in particular, in the limiting case of the PNLM (that occurs as $\xi \to 0$), we consider an asymptotic expansion in the small parameter ε.

4. Asymptotic solution of the boundary-value problems

Following a standard asymptotic argument (Kevorkian and Cole, 1996; Mikhasev et al., 2018) and similarly to the extraction of the edge effect in shells (Gol'denveizer, 1961; Kaplunov and Nobili, 2017), we seek a solution of the eigenvalue problem through superposition of a solution, $w^{(m)}$, valid in the interior of the beam (the so-called outer solution), with a pair of boundary layers, $w_1^{(e)}$ and $w_2^{(e)}$, fading off away from the left and from the right beam end, respectively,

$$w(s,\varepsilon) = w^{(m)}(s) + \varepsilon^{\gamma_1}w_1^{(e)}(s,\varepsilon) + \varepsilon^{\gamma_2}w_2^{(e)}(s,\varepsilon), \tag{21}$$

where $\gamma_{1,2} > 0$ and we have the order relations

$$\frac{\partial w^{(m)}}{\partial s} \sim w^{(m)}, \quad \frac{\partial w_i^{(e)}}{\partial s} \sim \varepsilon^{-\varsigma}w_i^{(e)} \quad \text{as} \quad \varepsilon \to 0.$$

The parameter ς is named *the index of variation of the edge effect integrals*, while $\gamma_{1,2}$ are the *indices of intensity of the edge effect integrals* near the left and right ends, respectively. The indices $\gamma_{1,2}$ depend on the boundary conditions and should be specified for each end.

4.1. Boundary layer

To derive an equation describing the behaviour of the solution in the vicinity of the ends (boundary layer), we zoom in by assuming $s = \varepsilon^{\varsigma}\sigma$ and $1-s = \varepsilon^{\varsigma}\sigma$, respectively for the left and for the right end. For either case, one obtains the distinguished limit $\varsigma = 1$ and Eq. (10) is rewritten as

$$\xi\frac{\mathrm{d}^6w_i^{(e)}}{\mathrm{d}\sigma^6} - \left(1-\varepsilon^2\theta\lambda^4\right)\frac{\mathrm{d}^4w_i^{(e)}}{\mathrm{d}\sigma^4} - \varepsilon^2\lambda^4\left(\theta+\varepsilon^2\right)\frac{\mathrm{d}^2w_i^{(e)}}{\mathrm{d}\sigma^2} + \varepsilon^4\lambda^4w_i^{(e)} = 0, \tag{22}$$

whose solution is sought in the form of an asymptotic series in the small parameter $\varepsilon \ll 1$

$$w_i^{(e)} = w_{i0}^{(e)} + \varepsilon w_{i1}^{(e)} + \varepsilon^2 w_{i2}^{(e)} + \ldots, \quad i = 1,2. \tag{23}$$

Substitution of (23) into (22) lends a sequence of differential equations in the unknowns $w_{ij}^{(e)}(\sigma)$, $i = 1,2$; $j = 0,1,2,\ldots$. Here, we simply give the first two terms of the expansion in the original variable s

$$w_1^{(e)}(s,\varepsilon) = a_{10}\mathrm{e}^{-\frac{s}{\varepsilon\sqrt{\xi}}} + \varepsilon\mathrm{e}^{-\frac{s}{\varepsilon\sqrt{\xi}}}\left[a_{11} + a_{10}\frac{\theta\lambda^4(1-\xi)}{2\sqrt{\xi}}s\right] + O\left(\varepsilon^2\mathrm{e}^{-\frac{s}{\varepsilon\sqrt{\xi}}}\right),$$

$$w_2^{(e)}(s,\varepsilon) = a_{20}\mathrm{e}^{-\frac{1-s}{\varepsilon\sqrt{\xi}}} + \varepsilon\mathrm{e}^{-\frac{1-s}{\varepsilon\sqrt{\xi}}}\left[a_{21} + a_{20}\frac{\theta\lambda^4(1-\xi)}{2\sqrt{\xi}}(1-s)\right] + O\left(\varepsilon^2\mathrm{e}^{-\frac{1-s}{\varepsilon\sqrt{\xi}}}\right), \tag{24}$$

where $a_{ij}\,(i = 1,2;\, j = 0,1,2,\ldots)$ are constants that will be determined in the following from the boundary conditions.

4.2. The outer solution

The displacement $w^{(m)}$ as well as the eigenvalue λ are sought in the form of an asymptotic series

$$w^{(m)} = w_0 + \varepsilon w_1 + \varepsilon^2 w_2 + \dots,$$

$$\lambda = \lambda_0 + \varepsilon\lambda_1 + \varepsilon^2\lambda_2 + \dots. \tag{25}$$

The leading term in the series corresponds to the solution of the classical local problem and λ_0 is the classical eigenvalue. Substituting (25) into the governing Eq. (10) and equating coefficients of like powers of ε leads to the sequence of differential equations:

$$\sum_{j=0}^{k} \mathbf{L}_j w_{k-j} = 0, \quad k = 0, 1, 2, \dots, \tag{26}$$

where

$$\mathbf{L}_0 z = \frac{\mathrm{d}^4 z}{\mathrm{d}s^4} + \theta\lambda_0^4 \frac{\mathrm{d}^2 z}{\mathrm{d}s^2} - \lambda_0^4 z, \quad \mathbf{L}_1 z = -4\lambda_0^3\lambda_1 \mathbf{D}z, \quad \mathbf{D}z = z - \theta\frac{\mathrm{d}^2 z}{\mathrm{d}s^2},$$

$$\mathbf{L}_2 z = -\xi\frac{\mathrm{d}^6 z}{\mathrm{d}s^6} - \theta\lambda_0^4\frac{\mathrm{d}^4 z}{\mathrm{d}s^4} + \lambda_0^4\frac{\mathrm{d}^2 z}{\mathrm{d}s^2} - 2\lambda_0^2\big(3\lambda_1^2 + 2\lambda_0\lambda_2\big)\mathbf{D}z,$$

$$\mathbf{L}_3 z = -4\theta\lambda_0^3\lambda_1\frac{\mathrm{d}^4 z}{\mathrm{d}s^4} + 4\lambda_0^3\lambda_1\frac{\mathrm{d}^2 z}{\mathrm{d}s^4} - 4\lambda_0\big(\lambda_0^2\lambda_3 + \lambda_1^3 + 2\lambda_0\lambda_1\lambda_2\big)\mathbf{D}z, \dots$$

At leading order, one finds the homogeneous forth order ODE

$$\mathbf{L}_0 w_0 = 0, \tag{27}$$

whose general solution

$$w_0(s) = c_{01}\sin(\beta s) + c_{02}\cos(\beta s) + c_{03}\mathrm{e}^{-\alpha s} + c_{04}\mathrm{e}^{\alpha(s-1)}, \tag{28}$$

depends on the constants, c_{0i}, $i \in \{1, 2, 3, 4\}$, to be determined through the boundary conditions. However, the ODE (27) is subject to six boundary conditions and the problem is to determine which of these correspond to the outer solution and which pertain to the boundary layer (Kevorkian and Cole, 1996). The procedure of splitting the boundary conditions also gives the indices of intensity of the boundary layer, γ_1, γ_2, as well as the constants c_{0k}, a_{ij}. For this, one needs to insert the expansions (21), (24) and (25) into the boundary conditions and equate coefficients of like powers of ε, while imposing the following requirements:

- in the leading approximation, every end condition should be homogeneous and coincide with those of the classical local theory;
- the kth-order approximation generates two equations coupling the constants $a_{i(k-1)}$ with the previous order approximation $w_{k-1}(s)$ evaluated at the boundaries.

4.3. Beam with simply supported ends

Let both beam ends be simply supported (S-S conditions), as given by the boundary conditions (12) rewritten in differential form through Eqs. (16a) and (16b), together with the additional constraints (18). Substituting the expansions (21), (24) and (25) into these conditions, we determine the strength of either boundary layer: $\gamma_1 = \gamma_2 = 3$.

At leading order, we arrive at the homogeneous classical boundary conditions

$$w_0(0) = w_0(1) = w_0''(0) = w_0''(1) = 0,$$

which give $c_{01} = C$, $c_{02} = c_{03} = c_{04} = 0$ and the classical eigenforms

$$w_0(s) = C\sin(\beta s), \quad \beta = \pi n, \quad n = 1, 2, \dots. \tag{29}$$

In light of the definition (20b), we find the eigenfrequencies

$$\lambda_0 = \lambda_0^{(n)} \equiv \frac{\pi n}{[1 + \theta(\pi n)^2]^{1/4}}, \qquad n = 1, 2, \dots, \tag{30}$$

and, using (9), the corresponding dimensional frequencies $\omega_0 = \sqrt{\frac{EI}{\rho S}}\,(\lambda_0/L)^2$.

Moving to first-order terms, we again obtain a set of homogeneous boundary conditions

$$w_1(0) = w_1(1) = w_1''(0) = w_1''(1) = 0, \tag{31}$$

as well as formulas for the leading amplitude in the boundary layer (24):

$$a_{10} = -\sqrt{\xi}\left(1 - \sqrt{\xi}\right)w_0'''(0) = C\beta^3\sqrt{\xi}\left(1 - \sqrt{\xi}\right), \tag{32a}$$

$$a_{20} = \sqrt{\xi}\left(1 - \sqrt{\xi}\right)w_0'''(1) = C(-1)^{n+1}\beta^3\sqrt{\xi}\left(1 - \sqrt{\xi}\right). \tag{32b}$$

Consideration of the inhomogeneous ODE (26) arising in this approximation, alongside the associated homogeneous boundary conditions (31), yields the compatibility condition $\lambda_1 = 0$, whence

$$w_1 = C_1\sin(\beta s),$$

where C_1 is an arbitrary constant. Without loss of generality, one can assume $w_1 \equiv 0$, for this amounts to taking $C = C_0 + \varepsilon C_1 + \dots$.

In the second-order approximation, when taking into account the outcomes of the previous step, we have again a homogeneous set of boundary conditions

$$w_2(0) = w_2(1) = w_2''(0) = w_2''(1) = 0, \tag{33}$$

and $a_{11} = a_{21} = 0$. The associated differential equation for w_2 reads

$$\mathbf{L}_0 w_2 = -\mathbf{L}_2 w_0 \equiv \xi\frac{\mathrm{d}^6 w_0}{\mathrm{d}s^6} + \theta\lambda_0^4\frac{\mathrm{d}^4 w_0}{\mathrm{d}s^4} - \lambda_0^3(\lambda_0 + 4\theta\lambda_2)\frac{\mathrm{d}^2 w_0}{\mathrm{d}s^2} + 4\lambda_0^3\lambda_2 w_0. \tag{34}$$

We thus arrive at the inhomogeneous boundary value problem (BVP) "on spectrum". Upon observing that the homogeneous BVP (33,34) arising at leading order is self-conjugated and therefore possesses the solution $z(s) = w_0(s)$, we deduce the compatibility condition

$$\int_0^1 w_0(s)\mathbf{L}_2 w_0(s)\mathrm{d}s = 0,$$

which readily gives the correction for the eigenvalue:

$$\lambda_2 = -\frac{\beta^2\big[\lambda_0^4\big(1 + \theta\beta^2\big) - \xi\beta^4\big]}{4\lambda_0^3\big(1 + \theta\beta^2\big)}.$$

On taking into account this result, Eq. (34) turns homogeneous and, without loss of generality, we can assume $w_2 \equiv 0$.

Considering the third-order approximation, one obtains the inhomogeneous boundary conditions

$$w_3(0) = -a_{10} = -C\beta^3\sqrt{\xi}\left(1 - \sqrt{\xi}\right),$$

$$w_3(1) = -a_{20} = C(-1)^n\beta^3\sqrt{\xi}\left(1 - \sqrt{\xi}\right),$$

$$w_3''(0) = \theta\lambda_0^4 a_{10} = C\theta\lambda_0^4\beta^3\sqrt{\xi}\left(1 - \sqrt{\xi}\right),$$

$$w_3''(1) = \theta\lambda_0^4 a_{20} = (-1)^{n+1}C\theta\lambda_0^4\beta^3\sqrt{\xi}\left(1 - \sqrt{\xi}\right) \tag{35}$$

for the inhomogeneous ODE

$$\mathbf{L}_0 w_3 = -\mathbf{L}_3 w_0 \equiv 4\lambda_0^3\lambda_3 \mathbf{D}w_0. \tag{36}$$

The compatibility condition for the BVP (35) and (36) works out

$$-w_3''(1)w_0'(1) + w_3''(0)w_0'(0) - w_3(1)w_0'''(1) + w_3(0)w_0'''(0)$$

$$+\theta\lambda_0^4\left[w_3(0)w_0'(0)-w_3(1)w_0'(1)\right]$$
$$+4\lambda_0^3\lambda_3\int_0^1\left(w_0-\theta w_0''\right)w_0\mathrm{d}s=0,$$

whence we get the next correction term for the eigenvalue

$$\lambda_3=\frac{\beta^6\sqrt{\xi}\left(1-\sqrt{\xi}\right)}{\lambda_0^3\left(1+\theta\beta^2\right)}. \tag{37}$$

The eigenform correction w_3, satisfying the boundary conditions (35), is given by the sum of a particular solution w_{3p} of Eq. (36), with the homogeneous solution w_{3o}. The former reads

$$w_{3p}(s)=C_{3p}\,s\cos(\beta s),$$

where

$$C_{3p}=2C\lambda_0^3\lambda_3\frac{1+\theta\beta^2}{\beta\left(\alpha^2+\beta^2\right)}=2C\frac{\beta^5}{\alpha^2+\beta^2}\sqrt{\xi}\left(1-\sqrt{\xi}\right).$$

Consequently, making use of (37), we get

$$w_3(s)=C\beta^3\sqrt{\xi}\left(1-\sqrt{\xi}\right)\{c_{32}\cos(\beta s)+c_{33}\exp(-\alpha s)+c_{34}\exp[\alpha(s-1)]-2c_{32}s\cos(\beta s)\},$$

with the constants

$$c_{32}=-\beta^2/\left(\alpha^2+\beta^2\right),$$
$$c_{33}=\tfrac{1}{2}\alpha^2\mathrm{e}^{\alpha}(1-\coth\alpha)[\mathrm{e}^{\alpha}+(-1)^n]/\left(\alpha^2+\beta^2\right),$$
$$c_{34}=-\tfrac{1}{2}\alpha^2\mathrm{e}^{\alpha}(1-\coth\alpha)[(-1)^n\mathrm{e}^{\alpha}+1]/\left(\alpha^2+\beta^2\right).$$

Breaking at this step the asymptotic procedure for seeking the eigenvalues λ_k and the associated eigenfunctions w_k, we obtain the asymptotic expansion

$$\lambda=\lambda_0\left[1-\tfrac{1}{4}\varepsilon^2\beta^2(1-\xi)+\varepsilon^3\beta^2\sqrt{\xi}\left(1-\sqrt{\xi}\right)+O\left(\varepsilon^4\right)\right],$$

where β and λ_0 are determined by Eqs. (29) and (30), respectively. Up to an undetermined factor, the associated eigenmode reads

$$w(s)=\sin(\pi n s)+\varepsilon^3(\pi n)^3\sqrt{\xi}\left(1-\sqrt{\xi}\right)\left\{c_{32}\cos(\pi n s)+c_{33}\exp(-\alpha s)+c_{34}\exp[\alpha(s-1)]-2c_{32}s\cos(\pi n s)+\exp\left(-\frac{s}{\varepsilon\sqrt{\xi}}\right)+(-1)^{n+1}\exp\left(\frac{s-1}{\varepsilon\sqrt{\xi}}\right)\right\}+O\left(\varepsilon^4\right). \tag{38}$$

It is of interest to compare the dimensional natural frequency, ω, determined with the TPNM, with its classical counterpart, ω_0, evaluated within the framework of local elasticity, i.e. for $\xi=1$. When taking into account the definition (9), we arrive at the relation

$$\frac{\omega}{\omega_0}=\left(\frac{\lambda}{\lambda_0}\right)^2=1-\frac{1}{2}\varepsilon^2(\pi n)^2(1-\xi)+2\varepsilon^3(\pi n)^2\sqrt{\xi}\left(1-\sqrt{\xi}\right)+O\left(\varepsilon^4\right). \tag{39}$$

Remarkably, this expression is independent of θ and this unexpected feature is indeed confirmed by the numerical solution of the TPNM, see Fig. 5. Fig. 1 plots the approximation (39) in the range $0<\xi<1$ against the numerical solution of the TPNM (given for $\xi>0.01$) for the scale parameter $\varepsilon=0.01, 0.05$ and 0.075. It appears that the 1-term asymptotic approximation is remarkably effective for small values of ε. The numerical solution of the TPNM given in Fig. 1 compares favourably with the corresponding solution depicted in Fig. 4 of (Fernández-Sáez et al., 2016) that, however, pertains to the range $\xi_1>0.1$, presumably owing to the numerical difficulties that may arise in the neighbourhood of the PNLM.

As a special case of Eq. (39), one obtains the eigenfrequency ratio corresponding to the PNLM (i.e. for $\xi=0$)

$$\frac{\omega}{\omega_0}=1-\frac{1}{2}\varepsilon^2(\pi n)^2+O\left(\varepsilon^4\right). \tag{40}$$

4.4. Beam with clamped ends

Consideration of a beam with clamped ends requires enforcing (11) and (18) on Eqs. (21),(24) and (25). We thus get the strength of the boundary layer $\gamma_1=\gamma_2=2$. In the leading approximation, one has the classical boundary conditions

$$w_0(0)=w_0(1)=w_0'(0)=w_0'(1)=0,$$

that give the constants

$$c_{01}=2\alpha(\cosh\alpha-\cos\beta)$$
$$c_{02}=2\alpha\sin\beta-2\beta\sinh\alpha,$$
$$c_{03}=\beta(\mathrm{e}^{\alpha}-\cos\beta)-\alpha\sin\beta,$$
$$c_{04}=-\mathrm{e}^{\alpha}\alpha\sin\beta+\beta(\mathrm{e}^{\alpha}\cos\beta-1), \tag{41}$$

as well as the frequency equation

$$\tfrac{1}{2}\theta\lambda_0^2\sin\beta\sinh\alpha+\cos\beta\cosh\alpha-1=0. \tag{42}$$

In particular, if $\theta=0$, one arrives at the classical frequency equation, $\cosh\lambda_0\cos\lambda_0=1$, valid for a Bernoulli–Euler beam, the corresponding eigenmode being

$$w_0(s)=C\left[U(\lambda_0\,s)-\frac{U(\lambda_0)}{V(\lambda_0)}V(\lambda_0\,s)\right],$$

where $S(x)$, $T(x)$, $U(x)$, $V(x)$ are the well-known Krylov–Duncan functions (Karnovsky and Lebed, 2010, § 14.4.3)

$$S(x)=\tfrac{1}{2}(\cosh x+\cos x),\ T(x)=\tfrac{1}{2}(\sinh x+\sin x),$$
$$U(x)=\tfrac{1}{2}(\cosh x-\cos x),\ V(x)=\tfrac{1}{2}(\sinh x-\sin x).$$

Besides, we get

$$a_{10}=\sqrt{\xi}\left(1-\sqrt{\xi}\right)w_0''(0), \tag{43a}$$

$$a_{20}=\sqrt{\xi}\left(1-\sqrt{\xi}\right)w_0''(1). \tag{43b}$$

In the first-order approximation, one has the inhomogeneous ODE (26)

$$\mathbf{L}_0w_1=4\lambda_0^3\lambda_1\mathbf{D}w_0, \tag{44}$$

and the procedure of splitting the boundary conditions gives

$$w_1(0)=w_1(1)=0, \tag{45a}$$

$$w_1'(0)=\left(1-\sqrt{\xi}\right)w_0''(0), \tag{45b}$$

$$w_1'(1)=-\left(1-\sqrt{\xi}\right)w_0''(1). \tag{45c}$$

The compatibility conditions for the BVP (44) and (45) reads

$$w_1'(1)w_0''(1)-w_1'(0)w_0''(0)-w_1(1)w_0'''(1)+w_1(0)w_0'''(0)-4\lambda_0^3\lambda_1\int_0^1\mathbf{D}w_0(s)w_0(s)\mathrm{d}s=0,$$

whence, accounting for Eq. (45), one obtains the correction

$$\lambda_1=-\lambda_0\frac{\left(1-\sqrt{\xi}\right)\left\{[w_0''(0)]^2+[w_0''(1)]^2\right\}}{4\int_0^1[w_0''(s)]^2\mathrm{d}s}, \tag{46}$$

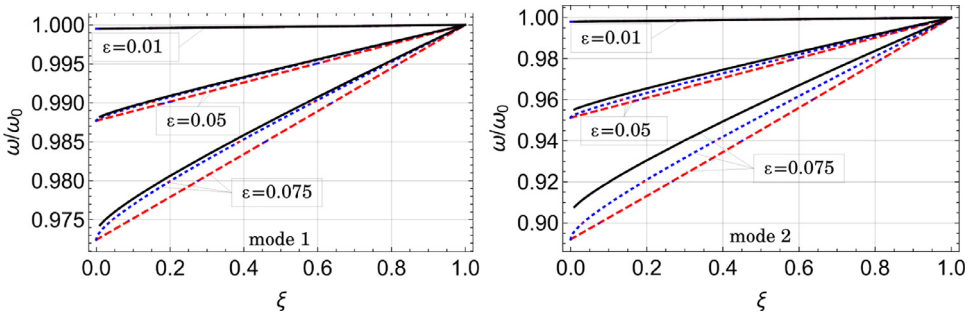

Fig. 1. 1st (left) and 2nd (right) eigenfrequencies ω for a S-S beam (solid, black), with $\varepsilon = 0.01$, 0.05 and 0.075, superposed onto the 1-term (dashed, red) and the 2-term (dotted, blue) asymptotic approximation, normalized with respect to the classical local frequency ω_0, Eq. (39). (For interpretation of the references to colour in this figure legend, the reader is referred to the web version of this article.)

where part-integration has been used at the denominator. Now, we can write the problem solution

$$w_1(s) = c_{11}\sin(\beta s) + c_{12}\cos(\beta s) + c_{13}e^{-\alpha s} + c_{14}e^{\alpha(s-1)} + w_{1p}(s), \tag{47}$$

where

$$w_{1p}(s) = 2\frac{\lambda_0^3\lambda_1}{\alpha^2+\beta^2}s\left\{\frac{1+\theta\beta^2}{\beta}[-c_{01}\cos(\beta s) + c_{02}\sin(\beta s)] + \frac{1-\theta\alpha^2}{\alpha}\left[c_{03}e^{-\alpha s} - c_{04}e^{\alpha(s-1)}\right]\right\} \tag{48}$$

is the particular solution of Eq. (44) with the coefficients c_{0j} being given by Eq. (41). In the special case of no rotational inertia, $\theta = 0$, Eq. (46) may be reduced to the very simple expression

$$\lambda_1 = -2\lambda_0\left(1-\sqrt{\xi}\right),$$

and Eq. (48) gives

$$w_{1p}(s) = \frac{\lambda_1}{\lambda_0}sw_0'(s) = -2C(1-\sqrt{\xi})\lambda_0 \times s\left[T(\lambda_0\, s) - \frac{U(\lambda_0)}{V(\lambda_0)}U(\lambda_0\, s)\right].$$

Similarly, Eq. (47) becomes

$$w_1(s) = C\left(1-\sqrt{\xi}\right)\lambda_0\left[T(\lambda_0\, s) - \frac{T(\lambda_0)}{V(\lambda_0)}V(\lambda_0\, s)\right] + w_{1p}(s).$$

Breaking the asymptotic procedure at this step, we can write down the approximate formula for the nonlocal-to-local frequency ratio

$$\frac{\omega}{\omega_0} = 1 - \tfrac{1}{2}\varepsilon\left(1-\sqrt{\xi}\right)\frac{\left[w_0''(0)\right]^2 + \left[w_0''(1)\right]^2}{\int_0^1\left[w_0''(s)\right]^2 ds} + O\left(\varepsilon^2\right), \tag{49}$$

that, in the absence of rotary inertia, reduces to

$$\frac{\omega}{\omega_0} = 1 - 4\varepsilon\left(1-\sqrt{\xi}\right) + O\left(\varepsilon^2\right). \tag{50}$$

Fig. 2 plots the approximated ratio (50) onto the numerical solution of the TPNM and shows that the 1-term correction provides excellent agreement for the fundamental mode. It is also clear from Eq. (50) that, as in the S-S situation, a perfectly reasonable limit is retrieved for the PNLM, i.e. for $\xi \to 0$.

The asymptotic expansion for the eigenmode reads

$$w = w_0 + \varepsilon w_1 + O\left(\varepsilon^2\right), \tag{51}$$

where w_0 and w_1 belong to the outer solution and they are given by (28), with coefficients (41), and by Eq. (47), respectively. We observe that the boundary layer terms are $O(\varepsilon^2)$ and therefore they do not appear explicitly in (51). To incorporate them consistently, one needs to consider the successive approximation term, $\varepsilon^2 w_2$, for the outer solution.

4.5. Beam with clamped and simply supported ends

To fix ideas, let the left beam end be clamped and the right simply supported. The correspondent boundary conditions are given by (11a), (12b) and the pair of additional conditions (18). In this case, we arrive at $\gamma_1 = 2$ and $\gamma_2 = 3$ for the left and for the right boundary layer, respectively.

At leading order, one has the classical boundary conditions

$$w_0(0) = w_0'(0) = w_0(1) = w_0''(1) = 0,$$

whence we get the constants in the general solution (28)

$$c_{01} = -2\lambda_0^2\left(\alpha^2\beta^{-2}\cosh\alpha + \cos\beta\right), \tag{52a}$$

$$c_{02} = 2\left(\lambda_0^2\sin\beta + \alpha^2\sinh\alpha\right), \tag{52b}$$

$$c_{03} = -\lambda_0^2\sin\beta - \beta^2\cos\beta - e^{\alpha}\alpha^2, \tag{52c}$$

$$c_{04} = e^{\alpha}\left(\beta^2\cos\beta - \lambda_0^2\sin\beta\right) + \alpha^2, \tag{52d}$$

together with Eq. (43a). The eigenvalues $\lambda_0 = \lambda_0^{(n)}$ are found from the transcendental equation

$$\alpha\cosh\alpha\sin\beta - \beta\cos\beta\sinh\alpha = 0,$$

that, when $\theta = 0$, boils down to

$$T(\lambda_0)U(\lambda_0) = S(\lambda_0)V(\lambda_0).$$

The last equation amounts to the well known classical equation $\tanh\lambda_0 = \tan\lambda_0$, while the correspondent eigenmodes are given by

$$w_0(s) = C\left[U(\lambda_0\, s) - \frac{S(\lambda_0)}{T(\lambda_0)}V(\lambda_0\, s)\right]. \tag{53}$$

The first-order approximation yields

$$w_1(0) = 0, \quad w_1'(0) = \left(1-\sqrt{\xi}\right)w_0''(0), \quad w_1(1) = w_1''(1) = 0, \tag{54}$$

and a_{10} and a_{20} are defined by Eqs. (43a) and (32b)

$$a_{10} = C\lambda_0^2\sqrt{\xi}\left(1-\sqrt{\xi}\right),$$

$$a_{20} = C\lambda_0^3\sqrt{\xi}(1-\sqrt{\xi})\left[V(\lambda_0) - \frac{S^2(\lambda_0)}{T(\lambda_0)}\right]. \tag{55}$$

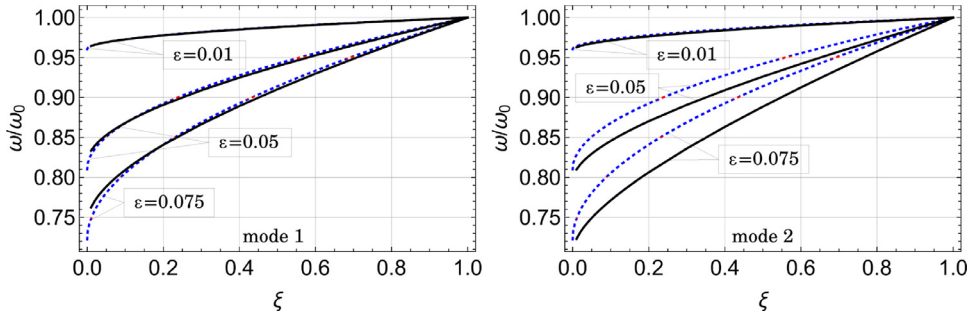

Fig. 2. 1st (left) and 2nd (right) eigenfrequencies ω for a C-C beam (solid, black) in the absence of rotatory inertia, $\theta = 0$, and with $\varepsilon = 0.01$, 0.05 and 0.075, superposed onto the 1-term (dotted, blue) asymptotic approximation, normalized with respect to the classical local frequency ω_0, Eq. (50). (For interpretation of the references to colour in this figure legend, the reader is referred to the web version of this article.)

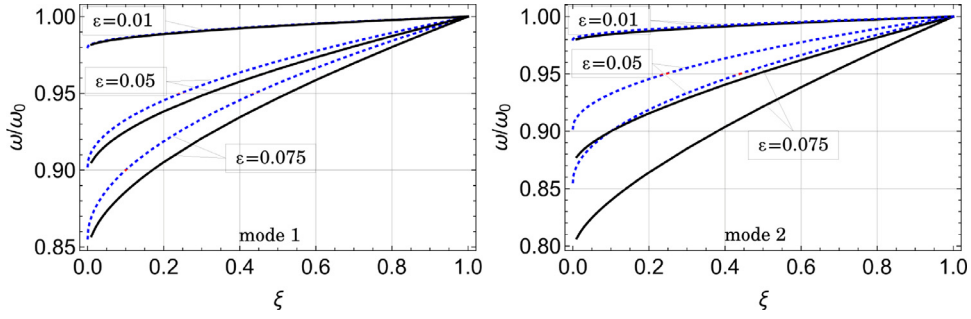

Fig. 3. 1st (left) and 2nd (right) eigenfrequencies ω for a C-S beam (solid, black) in the absence of rotatory inertia, $\theta = 0$, and with $\varepsilon = 0.01$, 0.05 and 0.075, superposed onto the 1-term (dotted, blue) asymptotic approximation, normalized with respect to the classical local frequency ω_0, Eq. (59). (For interpretation of the references to colour in this figure legend, the reader is referred to the web version of this article.)

The inhomogeneous Eq. (44), subject to the boundary conditions (54), possesses a solution provided that compatibility is satisfied, whereby we get the first eigenfrequency correction

$$\lambda_1 = -\lambda_0 \frac{\left(1-\sqrt{\xi}\right)[w_0''(0)]^2}{4\int_0^1 [w_0''(s)]^2 \mathrm{d}s}. \tag{56}$$

The solution of the BVP (44) and (54) has the form (47) as for the C-C case, yet with different coefficients. Indeed, in the special case $\theta = 0$, Eq. (56) simplifies to

$$\lambda_1 = -\lambda_0(1-\sqrt{\xi}),$$

and the particular solution becomes

$$w_{1p}(s) = \frac{\lambda_1}{\lambda_0} s\, w_0'(s) = C\lambda_1\, s\left[T(\lambda_0\, s) - \frac{S(\lambda_0)}{T(\lambda_0)} U(\lambda_0\, s)\right],$$

whence

$$\begin{aligned} w_1(s) &= C\lambda_0(1-\sqrt{\xi})\left[T(\lambda_0\, s) - \frac{S(\lambda_0)U(\lambda_0)}{T(\lambda_0)V(\lambda_0)} V(\lambda_0\, s)\right] + w_{1p}(s) \\ &= C\lambda_0(1-\sqrt{\xi})[(1-s)T(\lambda_0\, s) \\ &\quad + \frac{S(\lambda_0)}{T(\lambda_0)}\left(sU(\lambda_0\, s) - \frac{U(\lambda_0)}{V(\lambda_0)} V(\lambda_0\, s)\right)\Bigg]. \end{aligned} \tag{57}$$

Finally, we arrive at the following asymptotic expansion for the frequency ratio

$$\frac{\omega}{\omega_0} = 1 - \tfrac{1}{2}\varepsilon\left(1-\sqrt{\xi}\right)\frac{[w_0''(0)]^2}{\int_0^1 [w_0''(s)]^2 \mathrm{d}s} + O\left(\varepsilon^2\right) \tag{58}$$

that, in the case $\theta = 0$, reduces to

$$\frac{\omega}{\omega_0} = 1 - 2\varepsilon\left(1-\sqrt{\xi}\right) + O\left(\varepsilon^2\right). \tag{59}$$

Eq. (59) is plotted in Fig. 3 alongside the numerical solution of the TPNM. Although the accuracy of the expansion is restricted to small values of ε, we still appreciate a limit as the TPNM tends to the PNLM.

4.6. Cantilever beam

For a cantilever beam we have, at leading order,

$$w_0(0) = w_0'(0) = w_0''(1) = w_0'''(1) + \theta\lambda_0^4 w_0'(1) = 0,$$

and the constants in the general solution (28) are given by Eq. (52), i.e. they are the same as in the C-S case. The secular equation now reads

$$\left(1 + \tfrac{1}{2}\theta^2\lambda_0^4\right)\cosh\alpha\cos\beta - \tfrac{1}{2}\theta\lambda_0^2\sinh\alpha\sin\beta + 1 = 0,$$

that, in the special case of vanishing rotational inertia, reduces to

$$S^2(\lambda_0) - T(\lambda_0)V(\lambda_0) = 0.$$

This formula coincides with the classical result $\cosh\lambda_0\cos\lambda_0 + 1 = 0$ and the corresponding eigenforms are still given by Eq. (53).

In the first-order approximation, one arrives at the following boundary conditions

$$\begin{aligned} &w_1(0) = 0, w_1'(0) = \left(1-\sqrt{\xi}\right)w_0''(0), \\ &w_1''(1) = 0, w_1'''(1) + \lambda_0^4\theta w_1'(1) = -4\lambda_0^3\lambda_1\theta w_0'(1). \end{aligned} \tag{60}$$

together with the right boundary layer amplitude

$$a_{20} = \sqrt{\xi}\left(1-\sqrt{\xi}\right)\left[w_1''(1) + w_0'''(1)\right],$$

the left being given by Eq. (43a). The compatibility condition for the inhomogeneous BVP (44) and (60) is still given by Eq. (56) and, as a consequence, the eigenfrequency ratio (58) and the corresponding eigenmode correction are once again retrieved. Fig. 4 compares the normalized eigenfrequency ω/ω_0 as numerically evaluated for the TPNM with the 1-term expansion (59) and shows good accuracy. Besides, the numerical solution curve matches the corresponding result given in Fig. 5 of (Fernández-Sáez et al., 2016).

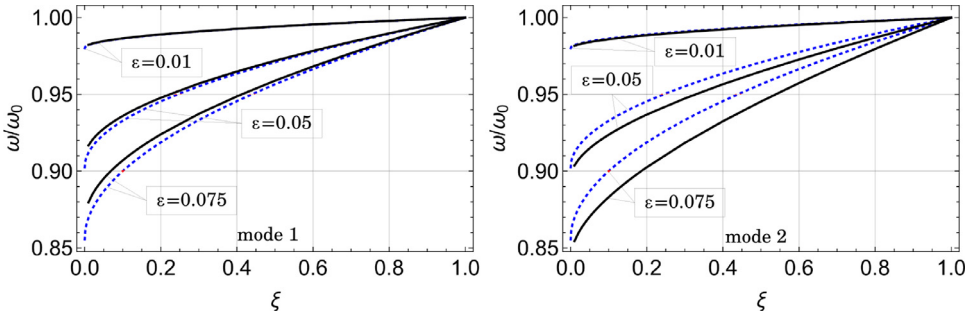

Fig. 4. 1st (left) and 2nd (right) eigenfrequencies ω for a cantilever beam (solid, black) in the absence of rotatory inertia, $\theta = 0$, and with $\varepsilon = 0.01$, 0.05 and 0.075, superposed onto the 1-term (dotted, blue) asymptotic approximation, normalized with respect to the classical local model frequency ω_0, according to Eq. (59). (For interpretation of the references to colour in this figure legend, the reader is referred to the web version of this article.)

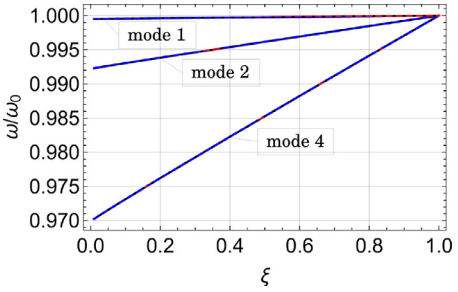

Fig. 5. Eigenfrequency ω for modes 1, 2 and 4 for a S-S beam, normalized over the classical frequency ω_0, for $\theta = 0, 1/100$ and $1/10$, as a function of the local model fraction ξ. As it occurs for the asymptotic expansion (39), the frequency ratio is unaffected by rotational inertia and curves overlap.

5. Purely nonlocal model

From the previous analysis, it clearly appears that the situation $\xi \to 0$ lends a perfectly admissible eigenfrequency which, therefore, can be assumed as the proper solution to the PNLM. We now consider what happens to the eigenmodes and for this we need to investigate the behaviour of the boundary layer term $B_\xi(s) = \sqrt{\xi}\exp[-s/(\varepsilon\sqrt{\xi})]$, $0 \le s \le 1$, as $\xi \to 0$. Clearly, this is a transcendentally small term for $s > 0$ and $B_\xi(s) \to 0$ uniformly. Non uniformity arises when we consider $s = 0$ for then a boundary layer appears that may be studied taking the rescaled variable $s^* = s/(\varepsilon\sqrt{\xi})$, see (Kevorkian and Cole, 1996). This boundary layer is vanishingly small as $\xi \to 0$ but not so are its derivatives with respect to s

$$B'_\xi(s) \to \begin{cases} 0, & s > 0, \\ -\varepsilon^{-1}, & s = 0, \end{cases} \quad \text{and} \quad B''_\xi(s) \to \begin{cases} 0, & s \neq 0, \\ +\infty, & s = 0, \end{cases}.$$

This result is the analogue of the steep boundary layer described in (Zhu and Dai, 2012) under static axial deformation. We may now ask whether this unboundedness in the second derivative leads to an unbounded bending energy. To answer this we first observe that $\forall \eta > 0$, $\int_0^\eta B''_\xi(s)\mathrm{d}s \to \varepsilon^{-1}$ uniformly and therefore $B''_\xi(s)$ is proportional to Dirac's delta function. Indeed, when considering the contribution M_ξ of the boundary layer B_ξ to the bending moment M through Eq. (4), we find

$$M_\xi(0) \to (2\varepsilon^2)^{-1},$$

at leading order. If we use this result in, say, the eigenmodes (38) for a S-S beam, we easily see that the boundary condition $M(0) = 0$ is satisfied at leading order, for the boundary layer cancels out the contribution of the outer solution. At the same time, the constitutive BCs are asymptotically satisfied for a vanishingly small ξ due to the asymptotic procedure applied above. We then conclude that, in the limit as $\xi \to 0$, the boundary layer warrants the fulfilment of all boundary conditions and it brings a finite contribution to the bending energy. From the standpoint of displacements, we get

$$w(s) \to w^{(m)} + \varepsilon^{\gamma_1 - 1} a_{10} R(-s) + \varepsilon^{\gamma_2 - 1} a_{20} R(s-1),$$

where $R(s)$ is the ramp function. For a S-S beam, we have $\gamma_1 = \gamma_2 = 3$ and

$$a_{10} = (-1)^{n+1} a_{20} = C\beta^3.$$

Whence, a finite jump in the rotation and a concentrated couple at the beam ends is produced. This is perhaps not so surprising, for solutions in the sense of distributions are to be expected when an integral form of the constitutive equation is adopted. Consequently, from a mathematical standpoint, an energy bounded solution of the PNLM may be consistently defined as the limit of the TPNM, although it is meaningful in the sense of distributions and we may want to reject it on physical grounds.

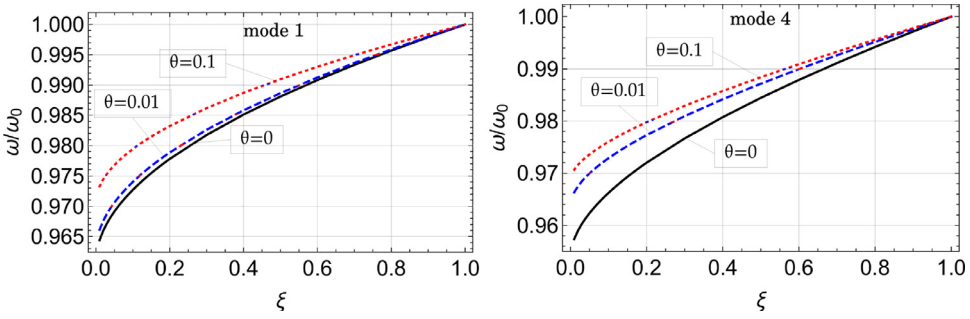

Fig. 6. Eigenfrequency ratio ω/ω_0 for modes 1 (left panel) and 4 (right) for a C-C beam for $\theta = 0$ (solid, black), $\theta = 1/100$ (dashed, blue) and 1/10 (dotted, red), as a function of the local model fraction ξ. (For interpretation of the references to colour in this figure legend, the reader is referred to the web version of this article.)

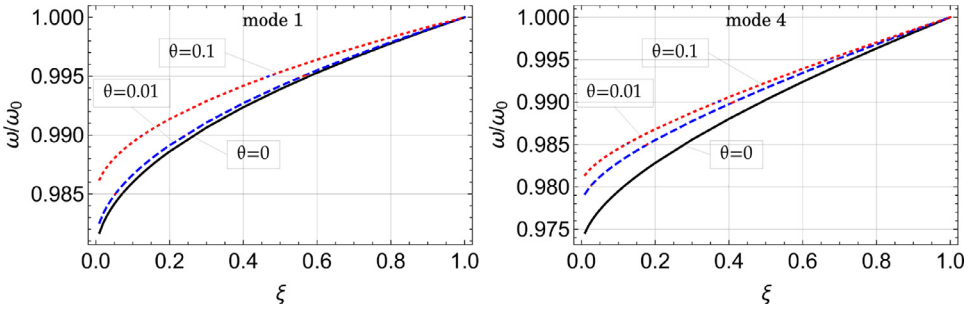

Fig. 7. Eigenfrequency ratio ω/ω_0 for modes 1 (left panel) and 4 (right) for a C-S beam for $\theta = 0$ (solid, black), $\theta = 1/100$ (dashed, blue) and 1/10 (dotted, red), as a function of the local model fraction ξ. (For interpretation of the references to colour in this figure legend, the reader is referred to the web version of this article.)

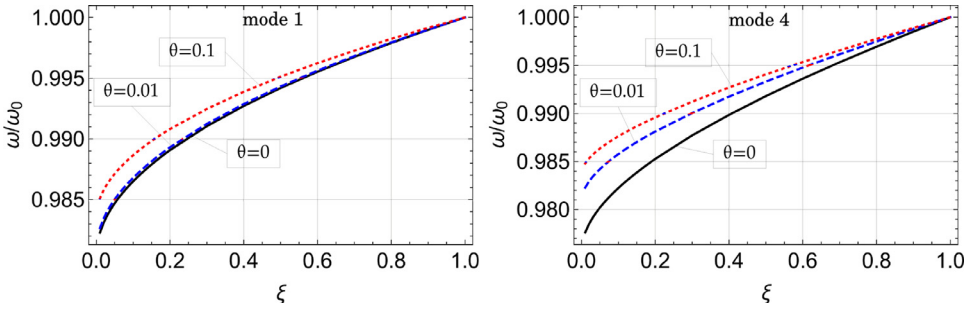

Fig. 8. Eigenfrequency ratio ω/ω_0 for modes 1 (left panel) and 4 (right) for a C-F beam for $\theta = 0$ (solid, black), $\theta = 1/100$ (dashed, blue) and 1/10 (dotted, red), as a function of the local model fraction ξ. (For interpretation of the references to colour in this figure legend, the reader is referred to the web version of this article.)

6. Influence of rotational inertia

We now consider the effect of including rotational inertia when considering the solution of the TPNM. For a S-S beam, Fig. 5 plots the eigenfrequency ratio ω/ω_0 for mode numbers $n = 1, 2$ and 4, with $\theta = 0,\ 1/100$ and 1/10. It appears that, for the S-S end conditions, rotational inertia is irrelevant for the purpose of determining the frequency ratio (yet it still affects ω_0). For a C-C beam, Fig. 6 plots the eigenfrequency ratio ω/ω_0 for mode numbers $n = 1$ and 4, with $\theta = 0,\ 1/100$ and 1/10. This time, rotational inertia plays an important role in the direction of contrasting the softening effect induced by the nonlocal fraction. Indeed, this hardening effect is already well manifest in the fundamental mode and, as expected, it becomes stronger for higher modes. Besides, encompassing rotational inertia of the cross-section has a significant bearing on higher modes, regardless of the actual value of θ. The same qualitative picture appears in Fig. 7 and in Fig. 8, respectively for C-S and C-F beams. It appears that the softening effect is stronger moving from S-S to C-C, C-F and then to C-S.

7. Conclusions

The purely nonlocal theory of beam elasticity has recently attracted considerable attention for the controversial results it conveys. Indeed, this model is believed to lead to ill-posed problems, owing to the appearance of a pair of constitutive boundary conditions which are generally incompatible with the natural boundary conditions. In this paper, we approach the problem from a different perspective and carry out an asymptotic analysis of the free vibrations of flexural beams endowed with rotational inertia, within the two-phase theory of nonlocal elasticity. We show that the nonlocal term contributes with a boundary layer whose strength greatly varies for different end conditions. In the case of simply supported beams, the boundary layer is the weakest and we provide a two-term correction for the classical solution. Remarkably, this situation is affected by the presence of rotational inertia only in the classical sense. Conversely, clamped-clamped, clamped-supported and clamped-free (i.e. cantilever) conditions bring a much stronger boundary layer, a for these we provide a single correction term. Numerical results confirm the accuracy of the asymptotic approach and show that rotational inertia is very relevant in contrasting the softening effect connected to the nonlocal phase. Most interestingly, for any end condition, the asymptotic solution still exists and its energy remains bounded in the limit of the purely nonlocal theory, that is for a vanishingly small local phase. This is in contrast to what is anticipated in the literature, see, for instance, Romano et al. (2017). We are therefore in the position of attaching a meaning to the purely nonlocal theory, as the limit of the two-phase theory. In so doing, we encounter a solution that is defined in the sense of distributions (for the curvature) and that, although questionable from a physical standpoint, is mathematically sound. This result is quite general for it extends to statics and, presumably, to axial vibrations in a rod.

Declaration of Competing Interest

The authors declare that they do not have any financial or non-financial conflict of interests.

Acknowledgements

GM gratefully acknowledges a Visiting Professor Position granted by the University of Modena and Reggio Emilia in the AY 2018/2019.

AN welcomes support from FAR2019, Piano di sviluppo dipartimentale DIEF, DR nr. 498/2019.

Supplementary material

Supplementary material associated with this article can be found, in the online version, at doi:10.1016/j.ijsolstr.2019.10.022.

References

Altan, S.B., 1989. Uniqueness of initial-boundary value problems in nonlocal elasticity. Int. J. Solids Struct. 25 (11), 1271–1278. ISSN 0020-7683.

Challamel, N., Wang, C.M., 2008. The small length scale effect for a non-local cantilever beam: a paradox solved. Nanotechnology 19 (34), 345703.

Cosserat, E., Cosserat, F., 1909. Théorie des Corps Déformables. Herman et Flis, Paris.

Dai, T.M., 2003. Renewal of basic laws and principles for polar continuum theories (i) micropolar continua. Appl. Math. Mech. 24, 1119–1125.

Eltaher, M.A., Khater, M.E., Emam, S.A., 2016. A review on nonlocal elastic models for bending, buckling, vibrations, and wave propagation of nanoscale beams. Appl. Math. Model. 40 (5–6), 4109–4128.

Eptaimeros, K.G., Koutsoumaris, C.C., Tsamasphyros, G.J., 2016. Nonlocal integral approach to the dynamical response of nanobeams. Int. J. Mech. Sci. 115, 68–80.

Eringen, A.C., 1983. On differential equations of nonlocal elasticity and solutions of screw dislocation and surface waves. J. Appl. Phys. 54 (9), 4703–4710.

Eringen, A.C., 1984. Theory of nonlocal elasticity and some applications. Technical report. Princeton Univ NJ Dept of Civil Engineering.

Eringen, A.C., 2002. Nonlocal Continuum Field Theories. Springer Science & Business Media.

Fernández-Sáez, J., Zaera, R., 2017. Vibrations of Bernoulli-Euler beams using the two-phase nonlocal elasticity theory. Int. J. Eng. Sci. 119, 232–248.

Fernández-Sáez, J., Zaera, R., Loya, J.A., Reddy, J.N., 2016. Bending of Euler–Bernoulli beams using Eringen's integral formulation: a paradox resolved. Int. J. Eng. Sci. 99, 107–116.

Gol'denveizer, A.L., 1961. Theory of thin elastic shells. International Series of Monograph in Aeronautics and Astronautics. Pergamon Press, New York.

Kaplunov, J., Nobili, A., 2017. A robust approach for analysing dispersion of elastic waves in an orthotropic cylindrical shell. J. Sound Vib. 401, 23–35.

Karnovsky, I.A., Lebed, O., 2010. Advanced Methods of Structural Analysis. Springer Science & Business Media.

Kevorkian, J., Cole, J.D., 1996. Multiple scale and singular perturbation methods. volume 114 of Applied Mathematical Sciences. Springer-Verlag New York, Inc.

Koutsoumaris, C.C., Eptaimeros, K.G., 2018. A research into bi-Helmholtz type of nonlocal elasticity and a direct approach to Eringen's nonlocal integral model in a finite body. Acta Mech. 229 (9), 3629–3649.

Koutsoumaris, C.C., Eptaimeros, K.G., Tsamasphyros, G.J., 2017. A different approach to Eringen's nonlocal integral stress model with applications for beams. Int. J. Solids Struct. 112, 222–238.

Lu, P., Lee, H.P., Lu, C., Zhang, P.Q., 2006. Dynamic properties of flexural beams using a nonlocal elasticity model. J. Appl. Phys. 99 (7), 073510.

Mahmoud, F.F., 2017. On the nonexistence of a feasible solution in the context of the differential form of Eringen's constitutive model: a proposed iterative model based on a residual nonlocality formulation. Int. J. Appl. Mech. 9 (07), 1750094.

Maugin, G.A., 2011. A historical perspective of generalized continuum mechanics. In: Mechanics of Generalized Continua. Springer, pp. 3–19.

Meng, L., Zou, D., Lai, H., Guo, Z., He, X., Xie, Z., Gao, C., 2018. Semi-analytic solution of Eringen's two-phase local/nonlocal model for Euler–Bernoulli beam with axial force. Appl. Math. Mech. 39 (12), 1805–1824.

Mikhasev, G., Avdeichik, E., Prikazchikov, D., 2018. Free vibrations of nonlocally elastic rods. Math. Mech. Solids 888–896. doi:10.1177/1081286518785942.

Mikhasev, G.I., 2014. On localized modes of free vibrations of single-walled carbon nanotubes embedded in nonhomogeneous elastic medium. ZAMM 94 (1–2), 130–141.

Mikhasev, G.I., Botogova, M.G., 2016. Free localized vibrations of a long double-walled carbon nanotube introduced into an inhomogeneous elastic medium. Vestnik St. Petersb. Univ. 49 (1), 85–91.

Nobili, A., Lanzoni, L., 2010. Electromechanical instability in layered materials. Mech. Mater. 42 (5), 581–591. ISSN 0167–6636 doi: 10.1016/j.mechmat.2010.02.006.

Nobili, A., Radi, E., Vellender, A., 2019. Diffraction of antiplane shear waves and stress concentration in a cracked couple stress elastic material with micro inertia. J. Mech. Phys. Solids 124, 663–680.

Peddieson, J., Buchanan, R., McNitt, R.P., 2003. Application of nonlocal continuum models to nanotechnology. Int. J. Eng. Sci. 41 (3), 305–312.

Pietraszkiewicz, W., Eremeyev, V.A., 2009. On natural strain measures of the non–linear micropolar continuum. Int. J. Solids Struct. 46, 774–787.

Pisano, A.A., Fuschi, P., 2003. Closed form solution for a nonlocal elastic bar in tension. Int. J. Solids Struct. 40 (1), 13–23.

Polyanin, A., Manzhirov, A., 2008. Handbook of Integral Equations. CRC Press, New York.

Polyanin, A.D., Manzhirov, A.V., 1998. Handbook of Integral Equations. CRC press.

Rafii-Tabar, H., Ghavanloo, E., Fazelzadeh, S.A., 2016. Nonlocal continuum-based modeling of mechanical characteristics of nanoscopic structures. Phys. Rep. 638, 1–97.

Romano, G., Barretta, R., Diaco, M., de Sciarra, F.M., 2017. Constitutive boundary conditions and paradoxes in nonlocal elastic nanobeams. Int. J. Mech. Sci. 121, 151–156.

Smirnov, V.I., 1964. A Course of Higher Mathematics, vol. 1. Pergamon.

Wang, Q., Liew, K.M., 2007. Application of nonlocal continuum models to nanotechnology. Phys. Lett. A 363 (3), 236–242.

Wang, Y.B., Zhu, X.W., Dai, H.H., 2016. Exact solutions for the static bending of Euler–Bernoulli beams using Eringen's two-phase local/nonlocal model. AIP Adv. 6 (8), 085114.

Yang, F., Chong, A.C.M., Lam, D.C.C., Tong, P., 2002. Couple stress based strain gradient theory for elasticity. Int. J. Solids Struct. 39 (10), 2731–2743.

Zhu, X., Dai, H., 2012. Solution for a nonlocal elastic bar in tension. Sci. China Phys. Mech. Astron. 55 (6), 1059–1065.

Zhu, X., Wang, Y., Dai, H.-H., 2017. Buckling analysis of Euler–Bernoulli beams using Eringen's two-phase nonlocal model. Int. J. Eng. Sci. 116, 130–140.